QUARTZ FABRIC VARIATIONS ACROSS THE GREENSCHIST FACIES SHEAR ZONE SEPARATING THE ZERMATT-SAAS AND COMBIN OPHIOLITIC ZONES, UPPER VAL GRESSONEY, WESTERN ALPS

Elisa Savignano*,✉, Steven M. Reddy, Jed Bridges**** and **Stefano Mazzoli*****

* *Dipartimento di Geoscienze, Università di Padova, Italy.*
** *The Institute for Geoscience Research, Department of Applied Geology, Curtin University of Technology, Perth, Australia.*
*** *Dipartimento di Scienze della Terra, dell'Ambiente e delle Risorse (DiSTAR), Università di Napoli Federico II, Italy.*
✉ *Corresponding author, e-mail: elisa.savignano@studenti.unipd.it*

Keywords: *Electron backscatter diffraction (EBSD), shear strain, deformation mechanisms, mylonites, Val Gressoney, Western Alps.*

ABSTRACT

The Gressoney Shear Zone (GSZ) consists of a ca. 500 m thick, intensely deformed rock panel located at the top of the high-pressure ophiolitic rocks of the Zermatt-Saas Zone in the Western Alps. This greenschist-facies shear zone accommodated multiple non-coaxial deformation events with contrasting kinematics. In this study, detailed field mapping and structural analysis were integrated with the study of crystallographic preferred orientation (CPO) from mylonites associated with the GSZ. Quartz CPO displays a systematic variation across the shear zone: moving from the basal shear zone boundary, the c-axes pattern changes from type II cross-girdle distribution, to an asymmetric pattern characterized by clustering of c-axes on one side of the Z-direction (inclined single girdle), to a central cluster in the Y-direction. The observed CPO patterns are consistent with increasing shear strain toward the basal contact, which probably controls the transition from broad peripheral maxima indicative of basal <a> slip to an inclined single girdle with no maxima, which is indicative of prism <a> slip, and finally an elongate single maximum at the girdle centre produced by a combination of prism <a> and rhomb <a> slip. Our results further indicate that basal <a> slip is dominant in pure quartz domains, whereas with increasing proportion of second phases, prism <c> slip is activated. These features confirm that CPOs obtained from the almost pure quartzites analysed in most published studies, and generally associated with the activation of distinct slip systems controlled by temperature, cannot be straightforwardly applied to the analysis of heterogeneous shear zones and/or polymineralic mylonites. From a regional point of view, the structures observed in the field and the fabric analyses are consistent with top-to-the-SE extension post-dating subduction-related high-pressure metamorphism and collisional nappe stacking in the studied sector of the Western Alps.

INTRODUCTION

The collisional belt of the Western Alps comprises ophiolitic units (or 'zones' in Alpine geology terminology; see Dal Piaz et al., 2003, for a review; Fig. 1) of the Mesozoic Piedmont Ocean that have been affected by blueschist to eclogite facies metamorphism during Eocene subduction (Bearth, 1967; Dal Piaz and Ernst, 1978; Platt, 1986). In the upper Val Gressoney, a metamorphic discontinuity occurs between the Zermatt-Saas Zone and the tectonically overlying Combin Zone (Reddy et al., 1999; Fig. 2) of the Piemonte Unit. The occurrence of high-pressure (HP) - and locally ultra high-pressure (UHP) - conditions in the footwall unit, and a significant pressure gap (ca. 1.0 GPa) between the footwall and the hanging-wall units have been the subject of numerous studies. The Combin Zone in the hanging wall, although entirely in greenschist facies in our study area, is known to preserve elsewhere evidence of blueschist facies metamorphism (Bearth, 1967; Dal Piaz, 1999; Reddy et al., 2003). On the other hand, the Zermatt-Saas Zone in the footwall is characterized by eclogite-facies metamorphism (Barnicoat and Fry, 1986) and is locally coesite-bearing (at the Lake Cignana site; Reineke, 1991). Therefore, these ophiolitic nappes must have followed independent kinematic trajectories before their eventual coupling at shallow structural levels (which is recorded by a greenschist facies overprint, as documented in this paper).

According to Reddy et al. (2003), the Combin Zone and the overlying continental basement of the Gneiss Minuti Complex and Arolla Series form a ca. 500 m thick, intensely deformed rock panel which divides two less deformed blocks, namely the Zermatt-Saas Zone in its footwall and the Sesia-Dent Blanche Unit in its hanging wall (Fig. 2B). This intensely deformed rock panel is interpreted to represent a complex shear zone - the Gressoney Shear Zone (GSZ) - that accommodated multiple non-coaxial deformation events with contrasting kinematics. The base of the GSZ, above the contact with the Zermatt-Saas Zone, is locally marked by the Cime Bianche Unit, which is made of Mesozoic calcareous metasediments and Triassic quartzites (Reddy et al., 2003; Pleuger et al., 2007).

The nature of the tectonic contact between the Zermatt-Saas and the Combin Zones, and the mechanisms controlling the exhumation of HP and UHP rocks have been intensely investigated in field studies based on the Val Gressoney area. Early models of backthrusting (Milnes et al., 1981; Ellis et al., 1989) were later replaced by new interpretations, supported by detailed kinematic and timing information, involving major extensional deformation. It has been proposed that the Zermatt-Saas Zone was exhumed at 42-41 Ma mainly as a result of extensional tectonics characterized by top-to-the-SE kinematics (Ballèvre and Merle, 1993; Reddy et al., 1999), followed by top-to-the-NW thrusting at 39-37 Ma. These episodes were followed by renewed top-to-the-SE extensional shear (Reddy et al., 2003).

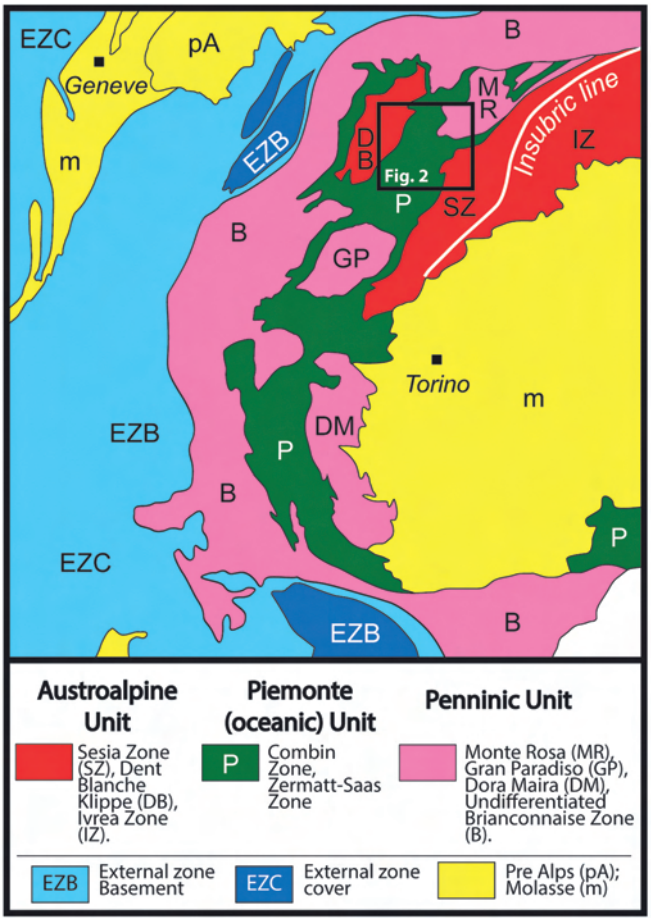

Fig. 1 - Simplified geological map of the Western Alps (after Reddy et al., 2003, modified). Marked area indicates the location of Fig. 2.

This study is focused on the basal part of the GSZ, close to the main boundary with the footwall high-pressure (HP) unit, in the upper Val Gressoney, Western Alps (Figs. 2 and 3). In order to provide a well constrained structural framework for the analysed shear zone sector, structural data (plotted in Fig. 4) were gathered from serpentinites located at the top of the Zermatt-Saas Zone, as well as from the Combin Zone calcschists and intercalated quartzites of the Cime Bianche Unit at the base of the GSZ. This latter was sampled in order to perform crystallographic preferred orientation (CPO) analysis. As undeformed rocks are usually characterized by randomly distributed lattice orientations of crystals, the occurrence of CPO provides an effective record of intracrystalline deformation and therefore its measurement is an important tool in microstructural studies. Different CPO patterns that develop are linked with the deformation history, which in turn strongly depends upon a series of parameters including temperature (Kruhl, 1998; Law, 2014), kinematics (Schmid and Casey, 1986; Boneh and Skemer, 2014; Cross et al., 2015), amount of strain (Heilbronner and Tullis, 2006), presence of fluids (e.g., Tullis et al., 1973), and presence of second phases (Hippertt, 1994). Therefore, CPOs can in principle be used to obtain information on several characteristics of the deformation including: (i) flow type (e.g., coaxial vs. non-coaxial strain), (ii) sense of local shear, (iii) amount and geometry of finite strain, (iv) temperature during deformation, and (v) dominant deformation mechanisms (e.g., Law et al., 1990). Studies on experimentally deformed quartzites demonstrated how CPOs development during crystal-plastic deformation is mainly based on the activation of different glide systems. The interaction with neighbouring crystals to accommodate the imposed strain may result in lattice rotations and thus in a re-orientation of crystallographic directions, providing a preferred orientation. Since critical resolved shear stress (CRSS) - which governs the activation of a particular slip system, and therefore influences CPO - is temperature-dependent (Hobbs, 1985), the link between temperature and CPO has been broadly investigated for quartz. In fact, it is well-known that the evolution of the CPO pattern of quartz c- and a-axis with increasing temperature (Passchier and Trouw, 1998; Stipp et al., 2002) is related to the sequential activation of various slip systems: basal <a> glide at low temperatures gives way to prism <a> slip with increasing temperature and, eventually, to dominant prism <c> slip (Blacic, 1975; Blumenfeld et al., 1986). Further controls on the c-axis pattern, associated with the type of flow, are also well understood, thanks to both experimental studies (Tullis et al., 1973; Tullis, 1977) and the analysis of naturally deformed quartzites (e.g., Price, 1985; Schmid and Casey, 1986; Pennacchioni et al., 2010; Kilian et al., 2011; Bestmann and Pennacchioni, 2015). More complications arise in the understanding of the effects of increasing strain; theoretically, it could lead to strengthening of the CPO pattern without changing the general shape (Lister and Hobbs, 1980). However, natural examples record a spatial transition of symmetrical cross-girdle to asymmetrical single girdles (Carreras and Celma, 1982; Schmid and Casey, 1986). This trend was found by Heilbronner and Tullis (2006) in a series of high-temperature experiments on quartz to moderate shear strains. More recently, Cross et al. (2015) showed a similar transition under increasing shear strain rates and stresses, in quartz layers deflecting around rigid porphyroclasts under isothermal conditions.

One of the main limitations in the previous works on CPO development arises from the fact that the examples are mainly pure quartzites and/or rocks deformed at laboratory conditions. In this study we analyse the development the CPO within a single, natural shear zone, focussing on the less known roles played by parameters such as shear strain and abundance of second phases as they act in natural systems. These factors have been analysed in few previous studies on quartz CPO (e.g., Hippertt, 1994; Heilbronner and Tullis, 2006; Little et al., 2015), as most works aimed at analysing fabric transitions - and the related activation of different slip systems in quartz - mainly as a function of temperature. Our results indicate that parameters other than temperature controlled marked variations of crystallographic fabrics observed in our samples, thus confirming that the estimation of deformation temperatures based on CPO patterns should be carried out with caution (e.g., Law et al., 2014).

THE STUDY AREA

The study area (Fig. 3) is dominated by outcrops of rocks of the Piemonte Unit. They lie structurally above the Monte Rosa Unit (Pennine Basement), which crops out only in the northern portion of the study area in a small, roughly round-shaped tectonic window. The Combin Zone consists of intercalated calcschists and metabasites, with a ca. 10 m thick quartzite unit (the Cime Bianche Unit) interbedded with calcschists close to the base of the unit. At the base of the Combin Zone, a ca. 50 m thick mylonitic serpentinite unit marks the contact with the underlying Zermatt-Saas Zone exposed in the central and northern portions of the mapped

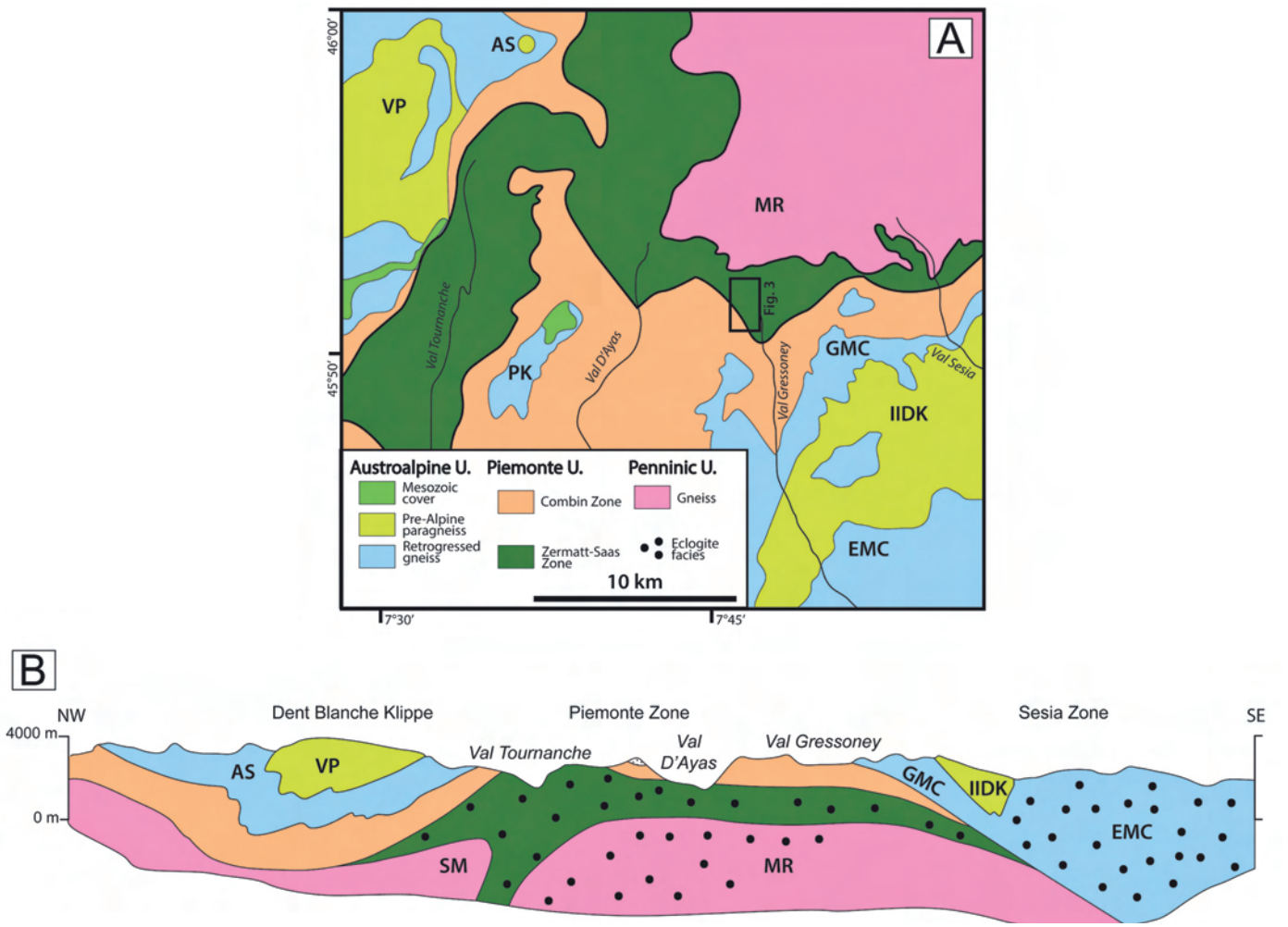

Fig. 2 - (A) Simplified geological map of the internal zones of the Western Alps north-west to the Aosta fault, showing location of Fig. 3 (after Reddy and Buchan, 2005, modified). The heavy line indicates the contact between oceanic eclogite- and greenschist-facies rocks that mark the base of the Gressoney Shear Zone. (B) Schematic cross-section through the Western Alpine internal zones. EMC- Eclogitic Micaschist Complex; GMC- Gneiss Minuti Complex; IIDK- Seconda Zona Diorito Kinzigitica; MR- Monte Rosa; AS- Arolla Schist; VP- Valpelline; PK- Pillonet Klippe; SM- Siviez-Mischabel Nappe.

area. Most of the Zermatt-Saas Zone exposed in the study area consists of serpentinites. These are in contact with metabasites to the east and to the north. The contact between the two lithologies dips to the west. To the south, the metabasites are bounded by metagabbros. The strike of this contact is NE-SW and is inferred to continue until it meets the Combin Zone in a triple junction.

Exhumed rocks of the Zermatt-Saas Zone in the study area include serpentinites, which preserve a HP mineral assemblage of antigorite + forsterite + magnetite ± clinohumite ± diopside, consistent with underplating in a subduction setting at eclogite-facies conditions.

The serpentinites of the Zermatt-Saas Zone feature a pervasive foliation and a pronounced mineral lineation. The foliation is defined principally by platy antigorite grains and strikes broadly NW-SE, being dominantly SW dipping (Fig. 4A). The lineation, defined by aligned elongated antigorite and clinohumite crystals and by magnetite stretching lineation, plunges dominantly to the west (Fig. 4A). Clinohumite lineation and antigorite lineation are consistently parallel to sub-parallel to magnetite stretching lineation. Magnetite lineation is more pronounced in retrogressed serpentinite outcrops. Kinematic indicators consist of S-C' fabrics and occasional σ-type porphyroclasts of pyroxene showing dominantly top-to-the-SE, and subordinately top-to-the-NW, sense of shear. Veins hosted in serpentinites are filled by antigorite, olivine and clinohumite. The veins show variable orientation across the mapped region (Fig. 4A). They either crosscut the main fabric, or are overprinted by it. Vein-filling antigorite fibres record an opening direction generally subparallel to the mineral/stretching lineation contained in the host rock for both the earlier and later generations. Metre-scale boudinage observed in the Zermatt-Saas Zone in the field area indicate flattening strain with bilateral extension in the XY-plane. Clinohumite is observed within the boudinaged competent layers. Late folding produced a mm-scale crenulation which pervasively overprints the main foliation of the Zermatt-Saas serpentinites and develops a crenulation cleavage. Fold axial planes strike dominantly NE-SW, dipping mostly to the NW, whereas fold hinge lines are more scattered but tend to plunge dominantly to the SW (Fig. 4D). Veins are also commonly folded. Notably, the metabasites of the Zermatt-Saas Zone contain no such overprinting late folds and crenulations, even where (e.g., in the southern part of the mapped area) they are adjacent to serpentinite outcrops displaying a well-developed crenulation. This suggests that late folding occurred in a zone of greenschist facies retrogression and strain localization.

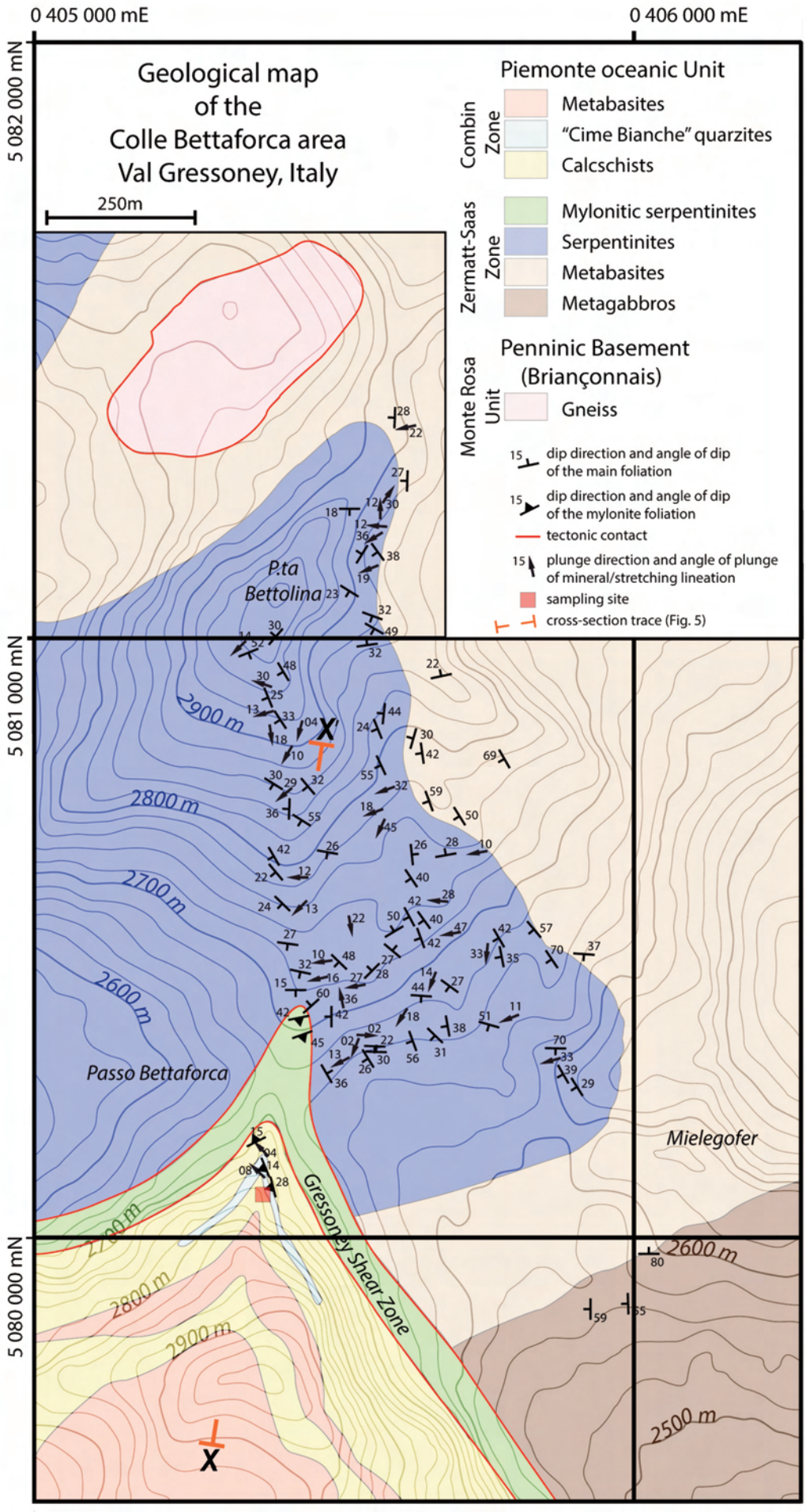

Fig. 3 - Geological map of field study area. The trace of the geological section X-X' shown in Fig. 5A is also indicated.

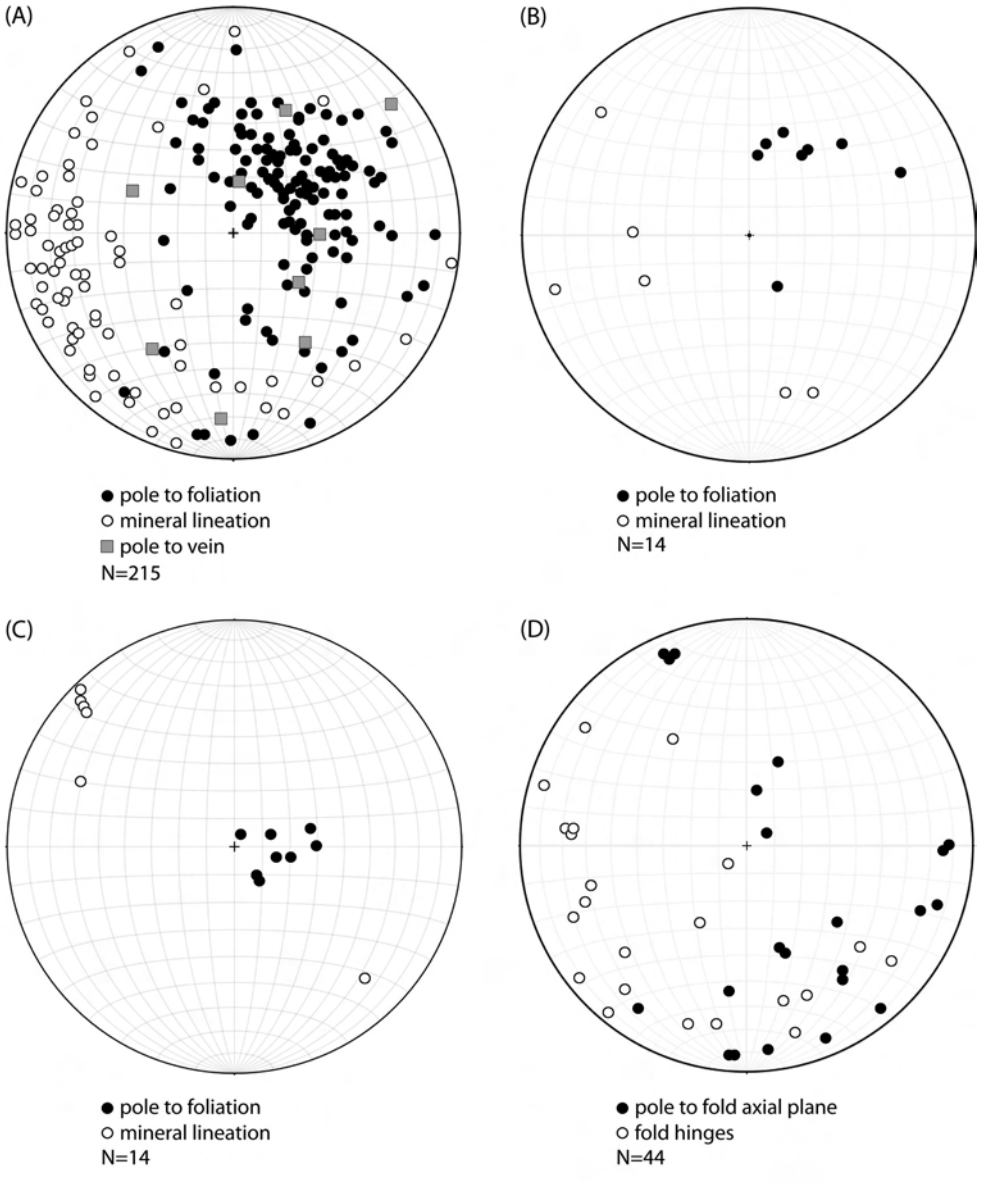

Fig. 4 - Orientation data (lower hemisphere, equal area projections; plots produced using the software OSX Stereonet; Allmendinger et al., 2011; Cardozo and Allmendinger, 2013). (A) Zermatt-Saas HP fabrics: poles to main foliation and extension veins, mineral lineation. (B) Zermatt-Saas greenschist-facies mylonitic serpentinites: poles to main foliation, mineral lineation. (C) Gressoney Shear Zone (metasediments): poles to main foliation, mineral lineation. (D) Zermatt-Saas late folds: poles to axial planes, hinge lines.

Consistently, the lower pressure serpentinite, which marks the contact between the Zermatt-Saas Zone and the overlying GSZ, contains an intense planar fabric consisting of a mylonitic foliation defined by the alignment of antigorite grains. This foliation strikes dominantly NW-SE and dips to the SW (Fig. 4B). The lineation is defined by aligned antigorite crystals and magnetite stretching lineation showing a variable orientation, broadly consistent with the westerly plunge of the lineation recorded from the bulk of the Zermatt-Saas serpentinites (compare Figs. 4A and 4B). Noticeably absent is the clinohumite-defined mineral stretching lineation as seen in the latter. The main foliation is affected by tight folds with angular hinge zones, and by an associated crenulation cleavage of variable intensity. Based on fold geometry, axial plane attitude and overprinting relationships, this late fold generation appears to be the same as that observed in the bulk of the Zermatt-Saas Zone HP serpentinites.

The basal part of the overlying GSZ is characterized by the occurrence of metasediments, dominantly represented by quartzites and calcschists. These rocks show a well-defined foliation characterized by westward gentle dips (Fig. 4C), particularly well developed in quartzites. Calcschists contain a mineral lineation defined by calcite, quartz and white mica, whereas quartzites contain a mineral lineation within the quartz matrix. The lineation plunges dominantly to the NW. No folding is observed in this basal part of the GSZ. Commonly shear bands and mica fish structures provide kinematic indicators recording top-SE directed movement.

MICROSTRUCTURAL ANALYSES: SAMPLE LOCATION AND METHODS

Six oriented samples were obtained from the calcschists located at the base of the Combin Zone and mainly from quartzites of the Cime Bianche Unit occurring within the GSZ and representing key horizons interposed between the Zermatt-Saas and the Combin Zones (Fig. 5A). Analyses in thin section included classic optical microscopy observations and mineral assemblage determination, while the percentage of quartz vs. other phases reported in Table 1 was defined on the basis of microcrystalline structure via Electron backscatter diffraction (EBSD; see below).

The cut surface devised for thin sections is parallel to lineation and perpendicular to foliation (i.e., the XZ-plane of the finite strain ellipsoid). Textural analyses were made using EBSD data collected by a Scanning Electron Microscopy (SEM) from four quartzo-feldspathic mylonites samples and two carbonate-bearing mylonite samples. Petrographic thin sections were treated for EBSD analyses at the Curtin University Department of Applied Geology. The standard procedure ensures the electron interaction with the specimen crystal lattice is able to produce Kikuchi bands which are used for identifying phases and for obtaining crystallographic orientations. First, thin sections were given a vibration polish using a colloidal silica polishing suspension on a Buehler Vibromet 2 (vibratory polisher). The duration of this polishing varied between 1 hour and 6 hours depending the mineralogy of the samples. Subsequently, they were coated with a thin layer of carbon to prevent surface charging in the SEM. The EBSD analysis was performed using a Zeiss Evo 40XVP SEM, fitted with a Nordlys EBSD camera. The main setup parameters included a tilt angle of 70°, a working distance of 15 mm, an accelerating voltage of 20 KeV, and a spot size of 550. Collection, crystallographic indexing and processing of EBSD patterns were carried out using the CHANNEL 5.10 Software by Oxford Instruments. Orientation data for grains is recorded using the Euler angle convention. The mean angular deviation (MAD) shows the angular misfit between the detected Kikuchi bands and the theoretical electron backscattering pattern (EBSP) for a particular phase. The MADs obtained for samples were typically good with values commonly around 0.6° (MAD over 1.3° indicates an erroneous result; Table 1). A variable step size of 3-20 μm was used. The data processing included noise reduction using a 'wildspike' correction, creating non-solutions for isolated indexed points, and a seven-neighbor zero solution extrapolation following standard procedures (Reddy et al., 2007). Orientation data were plotted with respect to the mesoscopic sample lineation and foliation (X-direction and XY-plane respectively), as lower hemisphere, equal area projections, using CHANNEL Mambo software. Orientation data were plotted as Pole Figures (PF). PFs for quartz c-axes were constructed for both all of the collected EBSD data ('all data') and as 'one point per grain data'. Contouring of plot represents multiples of a uniform distribution and uses a half width of 20° and a cluster size of 3°.

MICROSTRUCTURAL ANALYSES: RESULTS

The four samples collected from the Cime Bianche Quartzites (S11/10, S11/11, S11/12, S11/14; Fig. 6) are characterized by a mineral assemblage including quartz + microcline + white mica (phengite) ± rutile ± monazite ± apatite ± pyrite. A planar fabric is defined by a weak elongation of the quartz grains (e.g., S11/10CN), or locally by phengite (with quartz being more equant in shape; e.g., S11/14CN; Fig. 7). The grain size of the quartz matrix, although variable, is dominantly small (~ 20 μm). In particular, samples S11/12 and S11/15 show a strongly heterogeneous grain size and the presence of large K-feldspar crystals (Fig. 7). Sense of shear indicators are provided by structures, whose occurrence increases in the samples closer to the tectonic contact, including: (i) abundant σ-porphyroclasts, dominantly consisting of large (~ 200 μm) K-feldspar grains, (ii) mica fishes (white arrows in Fig. 7) uniformly interspersed within the matrix, and (iii) C'-type shear bands. The stair-stepping exhibited by the mica-fishes (ten Grotenhuis et al., 2003), σ-porphyroclasts and shear bands all point to a top-to-the-SE shear sense, consistent with kinematics identified in the field. Microcline showing a grain size similar to that of quartz also occurs randomly throughout the quartz matrix. Quartz exhibits undulose extinction and broad subgrain domains throughout the specimens, where mechanical Dauphiné twinning is also observed. The dominantly small grain size (~ 20 μm), common shape-preferred orientation and ubiquitous development of subgrains indicate that quartz in these samples has experienced widespread dynamic recrystallization. The two

Table 1 - EBSD post-processing parameters and sample position with respect to the main slip surface at the base of the GSZ.

	S11/10	**S11/11**	**S11/11B**	**S11/12**	**S11/13**	**S11/14**	**S11/15**
description	Quartzo-feldspathic mylonite	Quartzo-feldspathic mylonite	Quartzo-feldspathic mylonite	Quartzo-feldspathic mylonite	Carbonate mylonite	Quartzo-feldspathic mylonite	Carbonate-quartzo-feldspathic mylonite
#points	23400	43200	135000	25600	120000	66690	70000
Raster	180 x 130	180 x 240	450 x 300	160 x 160	400 x 300	342 x 195	350 x 200
Step size	20 μ	5 μ	5 μ	5 μ	4 μ	5 μ	4 μ
Zero solution	46.30%	21.40%	25.42%	37.92%	40.51%	38.19%	37.26%
Quartz	53.97%	78.60%	74.17%	62.08%	37.67%	61.81%	41.83%
Mean MAD	0.6648	0.5747	0.6017	0.6566	0.7503	0.6703	0.6506
grains	1195	620	1887	634	5694	1742	1229

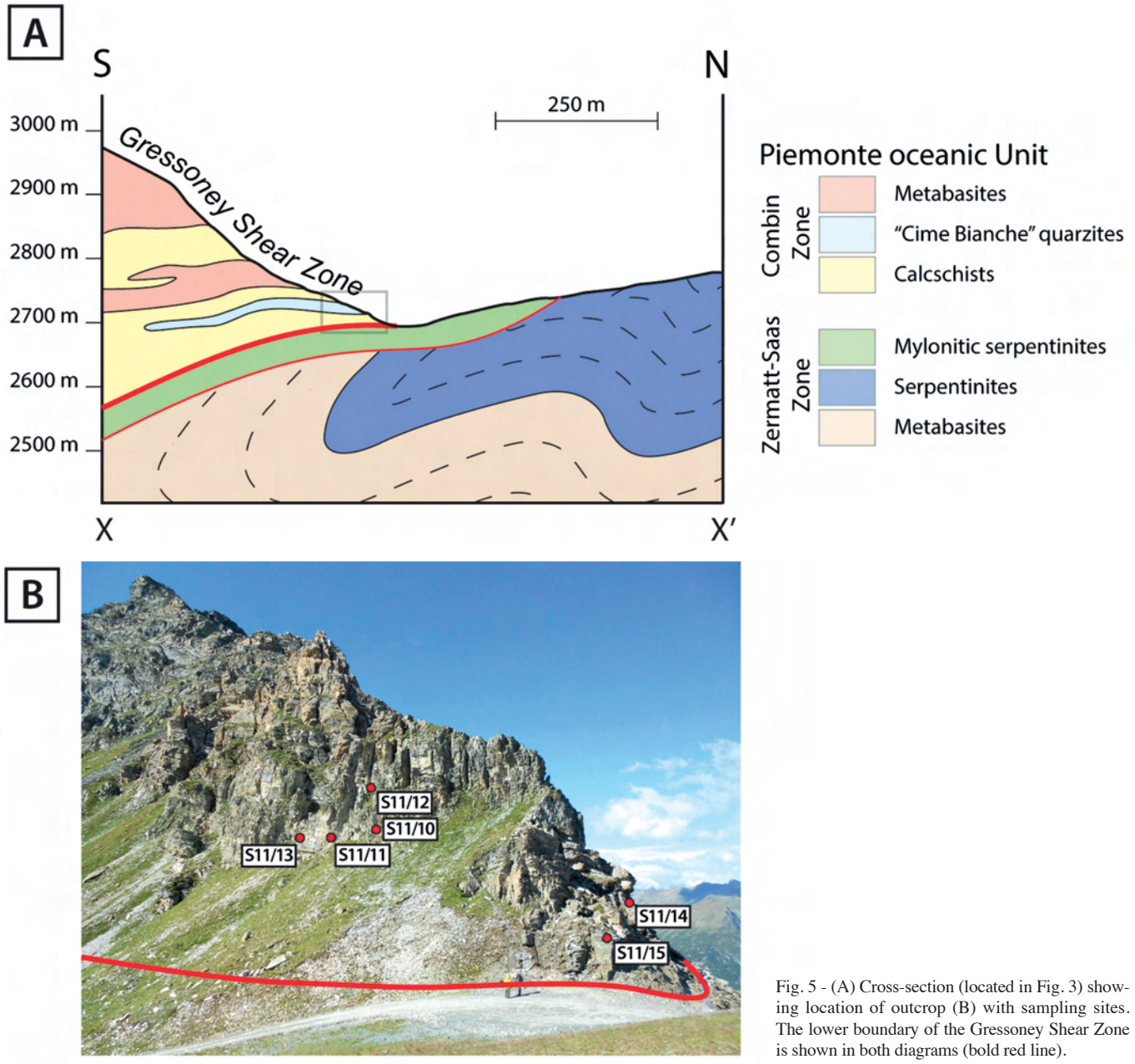

Fig. 5 - (A) Cross-section (located in Fig. 3) showing location of outcrop (B) with sampling sites. The lower boundary of the Gressoney Shear Zone is shown in both diagrams (bold red line).

samples (S11/13 and S11/15; Fig. 6) from Combin Calcschists show a typical mineral assemblage consisting mainly of calcite + dolomite and in minor proportion of quartz ± white mica ± phlogopite ± chloritoid (clinochlore/daphinite) ± K-feldspar ± rutile. Carbonates have variable grain size, with large calcite grains. Quartz represents ca. 38% (S11/13) and 42% (S11/15) (see Table 1) of the mineral phases occurring in these samples, where mica fishes are also observed (Fig. 7).

SEM-EBSD RESULTS

Most of the samples (i.e., S11/10, S11/11, S11/11B and S11/14) show strong similarities in Pole Figure (PF) between 'all data' and 'one point per grain data' plots (Fig. 8). In contrast, orientation data from S11/12 and S11/15 show an appreciable difference between plots of all of the collected EBSD data and single point per grain data because of the heterogeneous grain size and of the presence of large porphyroclasts. A strong preferred orientation occurs in all samples, indicating widespread intracrystalline deformation.

Quartz CPO in samples S11/10 and S11/12 forms a clear type II cross-girdle for c-axes, despite the different fabric strength for 'all data' and 'one point per grain data' plots for sample S11/12. Samples S11/11 and S11/11B are characterized by a strong asymmetric pattern, showing clustering of c-axes on one side of the Z-direction (inclined single girdle). In sample S11/13, a strong and atypical crystallographic preferred orientation sub-parallel to the X-direction is found. The CPO in sample S11/14 is dominated by a central cluster in the Y-direction. The pattern for S11/15 is characterized by a few clusters in the 'all data' plot; this pattern is controlled by the dominant occurrence of few large grains in the analysed portion of the thin section. For all the samples, no strong variation between +<a> and -<a> axes are recorded.

Misorientation axes PF (Fig. 8) are subdivided in ranges of misorientation angles of 1-2°, 2-5° and 5-10° respectively. For the majority of the samples, the rotation axes (< 10° of misorientation angle) lie parallel to the Y direction. This feature indicates a geometric control on the operation of different slip systems in grains of different orientations, with a rotation axis parallel to the crystal axis that is parallel to Y. The data are very systematic; only one sample (i.e., S11/13) does not follow this pattern, showing some degree of spread in the misorientation axis plot.

Two samples (S11/13 and S11/15) contain carbonates mixed in with quartz. One of them (S11/15) shows a c-axes preferred orientation forming an inclined single girdle on one side of the Z-direction in the 'one point per grain data' plot (which is more significant for this coarse grained sample).

A variation in c-axes patterns is clearly recognized in the PFs of Fig. 8, providing information about the dominant slip systems that operated in quartz (Fig. 9). For samples showing a cross-girdle pattern (S11/10 and S11/12), a combination of basal <a>, rhomb <a> and prism <a> systems may be inferred (Fig. 9A). On the other hand, a cluster near the Z-direction in samples S11/11 and S11/11B suggests the operation of basal <a> slip system. In sample S11/13, clustering sub-parallel to the X-direction is indicative of the activation of prism <c> slip. An elongate single maximum at the girdle centre produced by a combination of prism <a> and

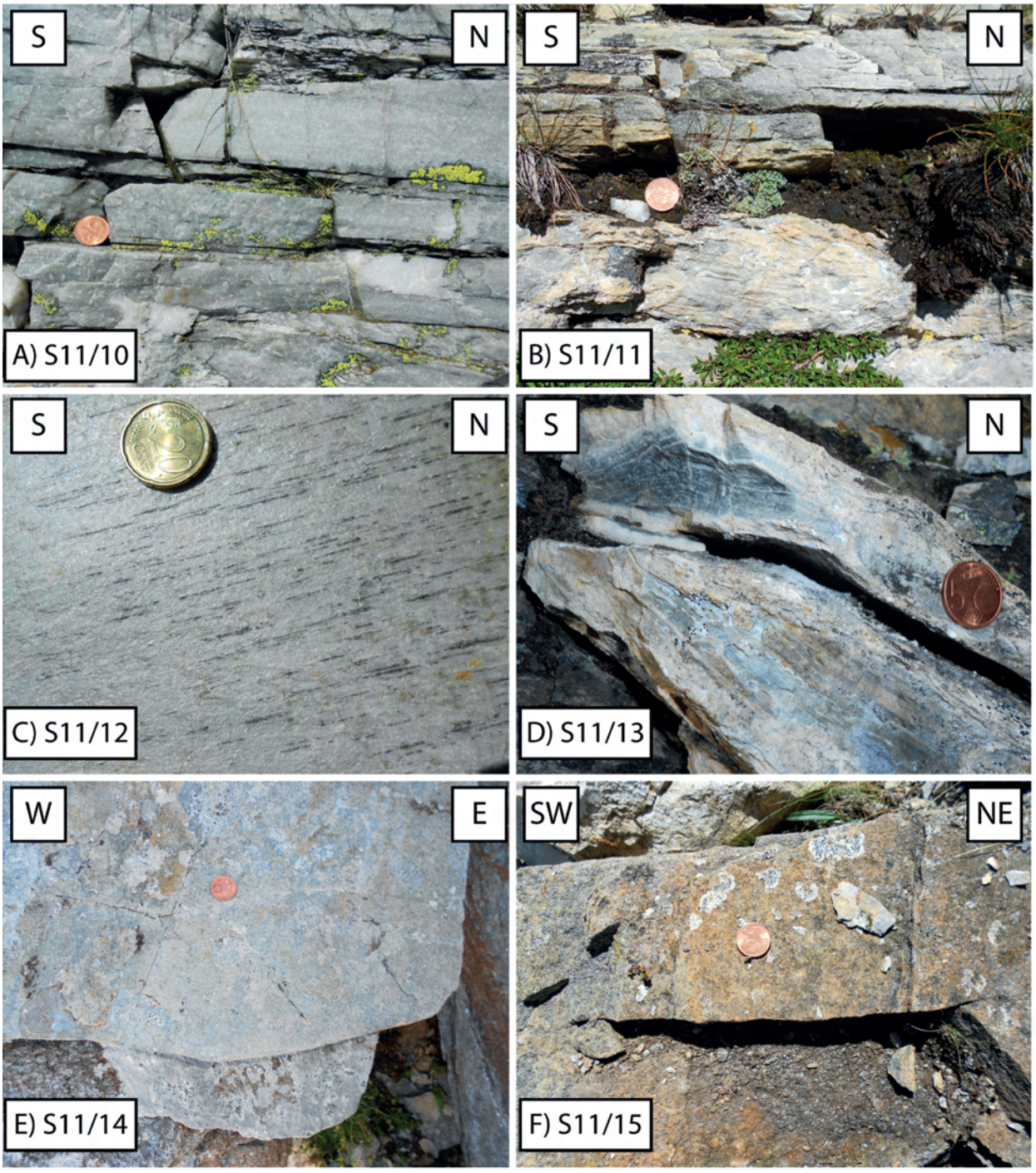

Fig. 6 - Photographs of the sampled lithotypes belonging to the Cime Bianche Quartzites (A, B, C, E) and Combin Calcschists (D, F).

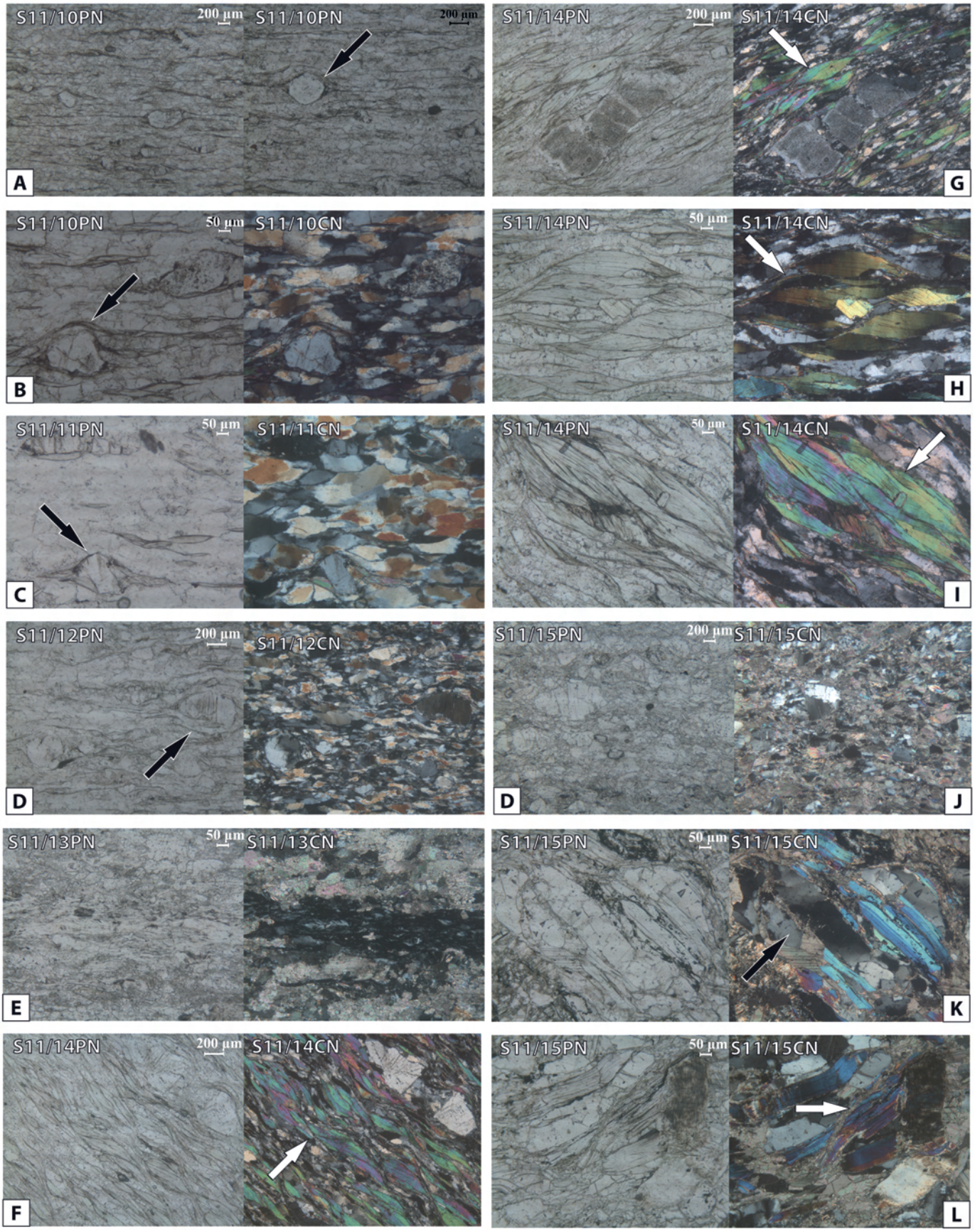

Fig. 7. Photomicrographs of the Cime Bianche quartzites (A, B, C, D, F, G, H, I) and the Combin Calcschists (E, J, K, L). PN- parallel nichols, CN- crossed nichols. Examples of kinematic indicators include rotated porphyroclasts (black arrows) and mica fish (white arrows).

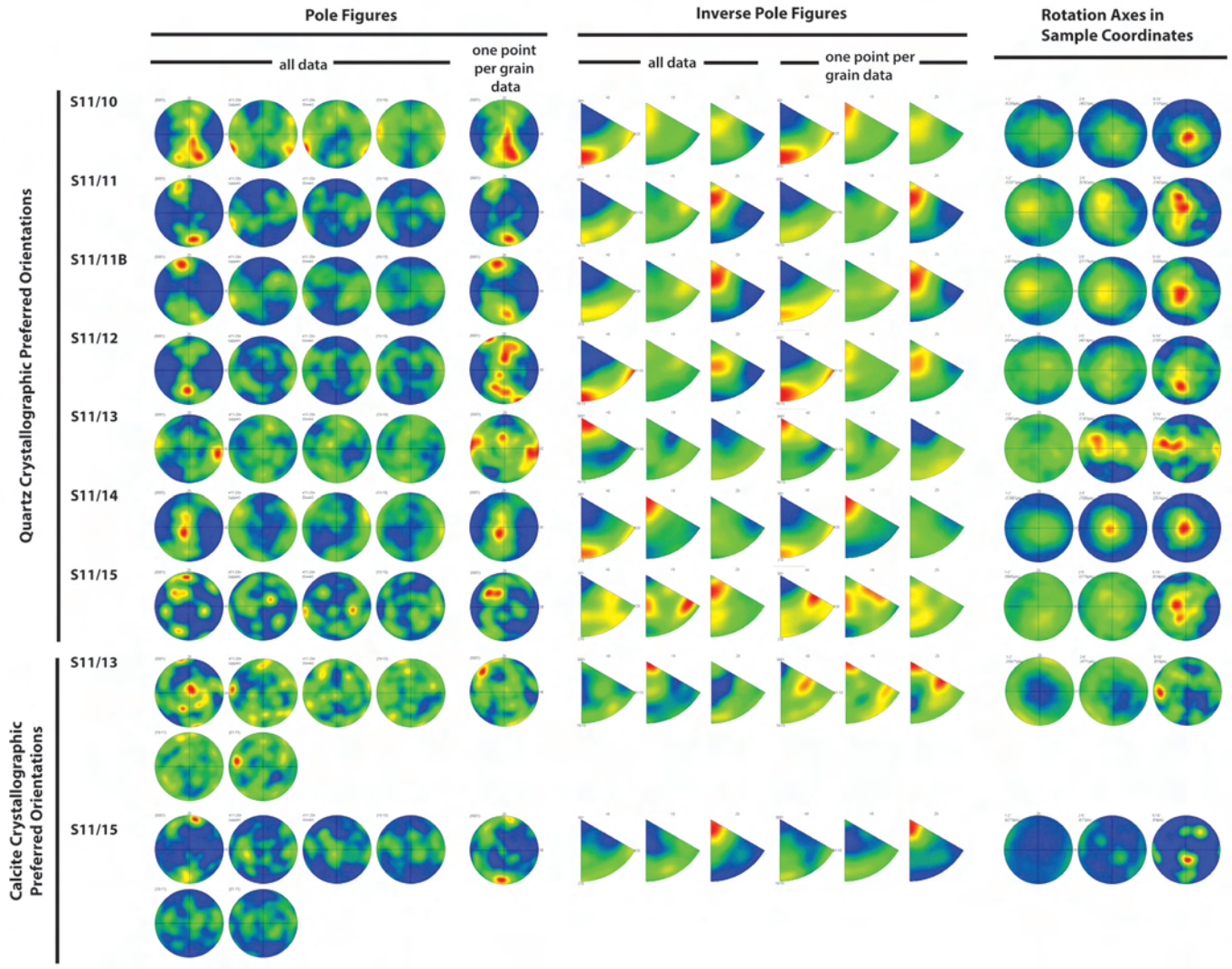

Fig. 8 - CPO diagrams showing Pole Figures, Inverse Pole Figures and Rotation Axes for all the samples, both for quartz and calcite. Pole Figures (lower hemisphere, equal-area projections) show contoured and point Pole Figures (with fabric skeletons on the latter), and < 10° neighbour-pair misorientation axes (SE to the right).

rhomb <a> slip is recorded in sample S11/14. Sample S11/15, dominated by few large grains, shows several clusters in the 'all data' plot; each cluster reflects the orientation of one of the grains, hence no significant information can be extracted from this sample.

The asymmetric c-axes pattern of calcite, which can be used as a kinematic indicator (Mazzoli et al., 2013, and references therein), is consistent with the top-to-the-SE sense of shear defined by S-C-C' fabrics and mica fish structures observed in thin section and suggested by quartz CPOs (e.g., samples S11/10, S11/12 and S11/14).

DISCUSSION

Fieldwork conducted on Zermatt-Saas serpentinites exposed in our study area unravelled structural assemblages consistent with the interpretations of superposed deformation proposed in previous studies (Reddy et al., 1999; 2003; Wheeler et al., 2001). A pervasive planar fabric is defined by the HP mineral assemblage and is related to early high strain. The lower pressure, higher strain mylonitic serpentinites that are found at the contact between the Zermatt-Saas Zone and the overlying Combin Zone, record retrogressive greenschist facies metamorphism that is attributed to localized deformation caused by the Gressoney Shear Zone. The overall top-to-the-SE sense of shear recorded by kinematic indicators in the study area supports a syn- to post-collisional extensional history of deformation, consistent with the models presented by Reddy et al. (1999; 2003). The GSZ encompasses the Combin Zone and the lower 100 m of the Gneiss Minuti Complex, and is partly responsible for the exhumation of the Zermatt-Saas eclogites in the footwall. The Zermatt-Saas serpentinites show a schistose fabric associated with an early high strain event related to the initial stages of exhumation during the Eocene (Reddy et al., 1999).

The main foliation and lineation detected by our fieldwork preserve a HP mineral assemblage of antigorite and clinohumite, recording eclogite facies conditions. The stretching direction of the HP minerals can be used as an indication of the principal strain orientation during the early stages of extension triggering tectonic exhumation. The orientation of the strain field in the later stages of extension can be inferred from the stretching direction exhibited by the lower pressure

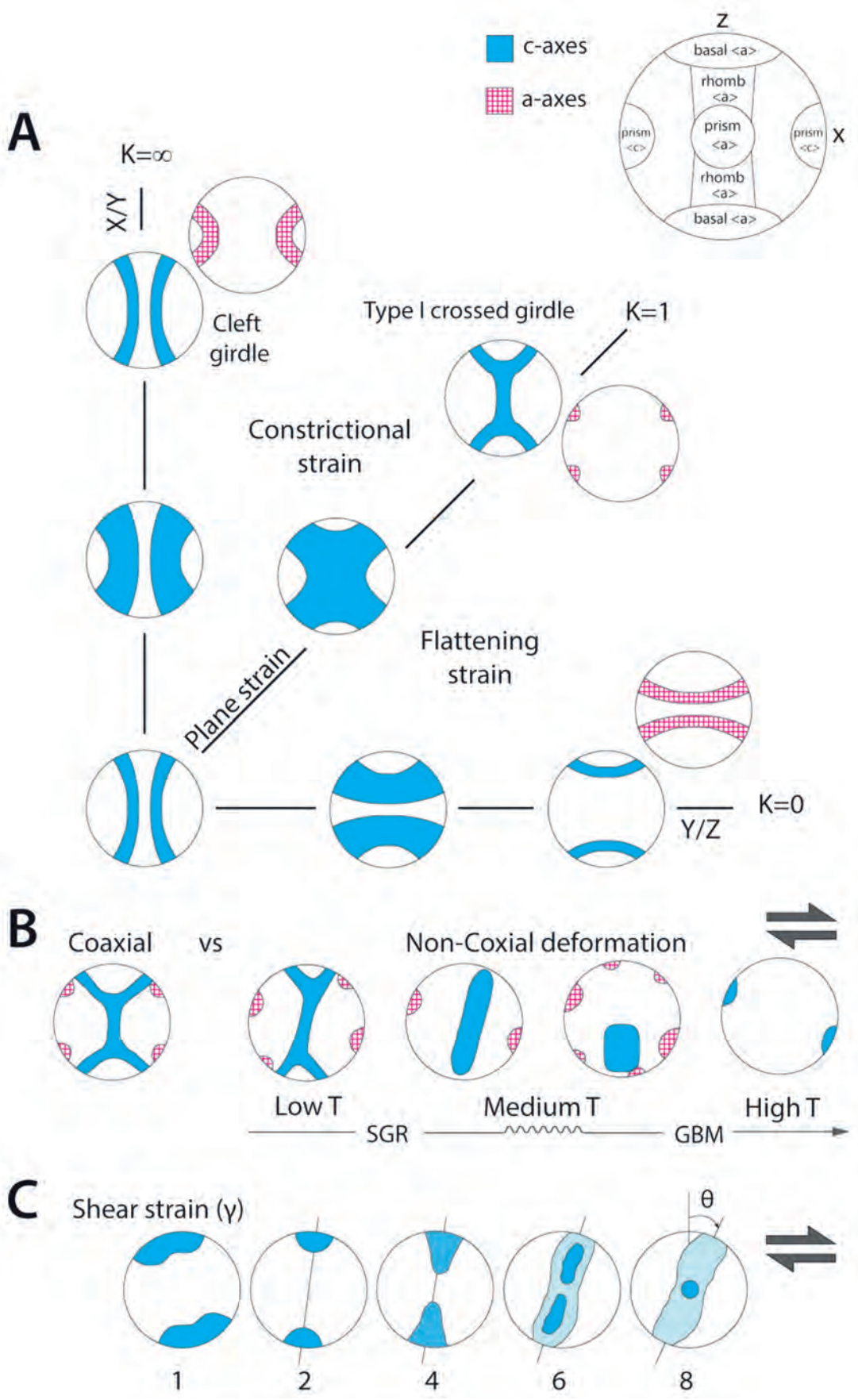

Fig. 9 - Theoretical CPO patterns in quartz as a function of various parameters (inset: slip systems corresponding to different quartz c-axis maxima; from Toy et al., 2008). (A) c- and a-axes distribution as a function of flow type (i.e. three-dimensional strain; after Passchier and Trouw, 1998, modified). (B) LPO diagrams expected for coaxial versus non-coaxial shear at different temperatures (after Passchier and Trouw, 1998, modified). (C) Pole Figure development as a function of increasing dextral shear strain (γ values, increasing to the right, are shown below each diagram; after Heilbronner and Tullis, 2005, modified).

mineral magnetite, which has crystallized at lower P-T conditions. The early high strain responsible for the main pervasive fabric of the serpentinites is a result of progressive deformation, as indicated by the relationships between the fabric and veins. Some veins are overprinted by the main fabric, whereas others cut the main foliation. In both generations, veins contain the same HP mineral assemblage seen in eclogite facies serpentinites. In addition, the mineral lineation defined by antigorite and clinohumite in the veins is sub-parallel to the mineral lineation of the host rock. This shows that the main strain event occurred as a progressive deformation, whose later stages were still characterized by high-pressure conditions. The HP fabrics are locally overprinted by greenschist facies metamorphism. In the field area, the Zermatt-Saas serpentinites are mostly seen to preserve eclogite facies metamorphism, although the mylonitic serpentinites show complete retrogression to greenschist facies. In fact, the mylonitic serpentinites adjacent to the lower boundary of the Combin Zone have experienced rehydration as exhumation progressed, with recrystallization of antigorite from clinohumite. Here, deformation is interpreted to have occurred at lower pressures but with a more intense and localized strain with respect to the bulk of the Zermatt-Saas Zone serpentinites, as it is evident from the reduced grain size produced by dynamic recrystallization during ductile flow.

The deformation unravelled by the present study can be bracketed in time using available radiometric constraints. Rb-Sr dating of mica grains from the GSZ indicates exhumation via extensional shear that occurred over a period of 9 Myr from ca. 45 Ma to ca. 36 Ma, overlapping with the eclogite facies conditions of the Zermatt-Saas Zone (Reddy et al., 1999; 2003). A metamorphic break of ca. 1.0 GPa is recorded across the tectonic contact (Reddy et al., 1999). Relics preserving blueschist facies metamorphism are in fact well known to occur regionally from the Combin Zone, although the rocks in the part of the hanging-wall unit analysed in this study are characterized exclusively by greenschist facies metamorphism. In fact, the GSZ accommodated crustal extension between c. 45 and 36 Ma, overlapping in time (or following) the eclogite facies metamorphic peak. Truncation of the greenschist fabric in the footwall is the proof that the eclogitic Zermatt-Saas Zone was already partly exhumed when the GSZ and the underlying eclogites were juxtaposed, implying that the GSZ is a late structure that did not control the initial stages of exhumation. Consequently, the metamorphic break is associated with the tectonic unroofing that brought the eclogites from c. 60 to c. 30 km depth, whereas removal of the remaining 30 km of overburden since 36 Ma appears to have been dominantly achieved by erosion (Reddy et al., 1999).

The results of this study, showing that the Cime Bianche Unit and Combin Calcschists sampled along the GSZ record greenschist facies conditions, are consistent with the interpretation of the GSZ as a late tectonic feature postdating substantial exhumation of the HP rocks.

Shear zone microstructures and crystallographic textures

Microstructures from Cime Bianche Quartzites and Combin Calcschists from the base of the GSZ, close to the tectonic contact with the underlying Zermatt-Saas Zone, record non-coaxial strain associated with top-to-the-SE shearing under greenschist facies conditions. Crystallographic fabrics analysed by SEM-EBSD record crystal plastic strain in both quartz and calcite. The presence of mica fish structures, C'-type shear bands and asymmetric mantled porphyroclasts, typical in high strain zones dominated by non-coaxial deformation, characterizes the samples closer to the tectonic contact. Undulose extinction and extensive subgrain development with broad subgrain domains suggest that dynamic recrystallization in quartz was dominated by subgrain rotation (SGR) mechanisms. This is consistent with the distribution of neighbour-pair misorientations (the misorientation data between neighbouring points in the maps), which shows a large number of low-angle (< 10°) misfit between adjacent points, misorientation axes being clustered around the Y-axis (Fig. 8). This suggests some form of crystallographic rotation, such as that by subgrain rotation.

The samples analysed in this study lie all within the basal part of the same shear zone, being located at a distance of few meters from each other (Table 1); they experienced similar P-T conditions during deformation, as it is also confirmed by their consistent greenschist facies mineral paragenesis and microstructure development. However, an increase in shear strain moving towards the basal contact may be assumed, as it is typical in heterogeneous simple shear zones (Ramsay and Huber, 1987) and in zones of 'general shear' (Vitale and Mazzoli, 2008; 2010). As a matter of fact, quartz CPOs obtained by EBSD analysis show a systematic variation across the shear zone (compare with Schmid and Casey, 1986). The samples more distant from the basal contact (S11/12 and S11/10) are characterized by a clear type II cross-girdle distribution of c-axes. Moving towards the basal contact, the type II cross-girdle distribution changes to an asymmetric pattern characterized by clustering of c-axes on one side of the Z-direction (inclined single girdle, S11/11 and S11/11B). Closer to the basal contact, a strong and atypical crystallographic preferred orientation sub-parallel to the X-direction is found in sample S11/13. Finally, the c-axis distribution in the sample (S11/15) closest to the basal contact is dominated by an inclined single girdle on one side of the Z-direction in the 'one point per grain data' plot of Fig. 8. The observed CPO patterns are consistent with increasing shear strain toward the basal contact, which probably controls the transition from broad peripheral maxima indicative of basal <a> slip to an inclined single girdle with no maxima indicative of prism <a> slip, and finally an elongate single maximum at the girdle centre produced by a combination of prism <a> and rhomb <a>.

Fig. 9 shows a summary of parameters that have been proposed to control quartz CPOs, including shape of the finite strain ellipsoid (Fig. 9A), as well as increasing temperature (Fig. 9B) and shear strain (Fig. 9C) within the general framework of non-coaxial deformation. The results presented in this study show a strong similarity with experimentally sheared quartzites, which display a similar transition of CPOs patterns with increasing shear strain (Heilbronner and Tullis, 2006; Muto et al., 2011; Fig. 9C). Furthermore, investigated natural examples of mylonites by both Toy et al. (2008) and Schmid and Casey (1986) show a comparable fabric transition across a single shear zone, indicating finite strain increase as the main responsible for the variation in fabric skeleton. Although for decades researchers have attempted to correlate fabric variations with temperature, within a general framework of non-coaxial deformation (e.g., Tullis et al., 1973; Blacic, 1975; Tullis, 1977; Hobbs, 1985; Blumenfeld et al., 1986; Law et al., 1990; Passchier and Trouw, 1998; Stipp et al., 2002; Law et al., 2014; Fig. 9B), the patterns obtained in this study from specimens located within a single

shear zone confirm that the operation of certain slip systems in quartz is not only a function of temperature - which is not likely to have varied significantly between our samples - and that further, less studied parameters (e.g., shear strain, presence of second phases) play a significant role. The fabric transition observed across the shear zone at the base of the Combin Unit in the upper Val Gressoney is consistent with previous studies (e.g., Pennacchioni et al., 2010; Kilian et al., 2011; Bestmann and Pennacchioni, 2015) indicating that deformation history and finite strain play an important role in fabric development. On one hand, clustering in the Y-direction - resembling HT patterns - may be explained by high shear strain values close to the main tectonic contact, as suggested by laboratory experiments (Heilbronner and Tullis, 2006). On the other hand, the anomalous pattern of quartz c-axes clustering sub-parallel to the X-direction observed in sample S11/13 suggests a strong control of second phases on CPO development. This sample, in fact, is characterized by a significant occurrence (62%) of minerals different from quartz. This is consistent with previous observations by Hippertt (1994) and Peternell et al. (2010) showing that, within a single mylonite, basal <a> slip is dominant in quartz in pure quartz domains, whereas with increasing proportion of second phases, prism <c> slip is activated, producing a pattern of quartz c-axes clustering sub-parallel to the X-direction (Fig. 8). This is also consistent with the concept of quartz behaving as a 'strong' phase when it occurs in polymineralic rocks, as opposed to its 'weak' behaviour (ease of flow) in pure quartzites (Menegon et al., 2008).

CONCLUSIONS

Shear sense indicators (at both outcrop- and micro-scale) from the study area record dominantly top-to-the-SE extensional kinematics of the GSZ, corroborating what documented by Reddy et al. (2003). The occurrence of large aggregates of clinohumite and antigorite observed in the field within the footwall serpentinite of Zermatt-Saas Zone is consistent with the high-pressure peak metamorphism (eclogite facies) characterising this unit. On the other hand, the mineral assemblage of the Combin Zone and Cime Bianche Unit in the basal part of the GSZ records a widespread greenschist facies overprint and does not preserve any relic of the blueschist facies paragenesis observed elsewhere in the Combin Unit (Bearth, 1967; Dal Piaz, 1999; Reddy et al., 2003). SEM-EBSD analysis, performed on previously petrographically analysed thin sections from the Combin and Cime Bianche Units, provide interesting results on the development and evolution of quartz CPO. The activity of the various slip systems in quartz in natural mylonites formed at constant (greenschist facies) P-T conditions appear to be correlated with the position within the shear zone. Moving toward the basal boundary of the GSZ, i.e., likely the zone of highest shear strain, a transition from broad peripheral maxima indicative of basal <a> slip to an inclined single girdle indicative of combined slip on prism <a>, rhomb <a> and basal <a> slip systems, and finally an elongate single maximum at the girdle centre produced by a combination of prism <a> and rhomb <a> slip is recorded. The observed fabric transition, rather than being produced by increasing temperature as it is commonly assumed to occur within a non-coaxial deformation regime (Fig. 9B), is in this case controlled by the proximity to the main tectonic contact. Therefore, such a transition among dominant slip systems in quartz is likely to be associated with increasing shear strain, which in this case appears to be the main controlling factor in the development of the fabric skeleton. Moreover, the activation of <c> prism slip observed in second phases-rich samples is consistent with the results of recent studies (Menegon et al., 2008; Peternell et al., 2010) unravelling the role of deformation partitioning in the behaviour of quartz. This mineral behaves as a "strong" phase when surrounded by a "weak" matrix, which leads to an apparently anomalous activation of <c> prism slip at temperatures significantly lower than those previously suggested based on experimental studies on quartz deformation (Tullis et al., 1973; Tullis, 1977). Therefore, the new results obtained in this study suggest that parameters other than temperature (e.g., shear strain, abundance of second phases) should be taken into account more thoroughly in the study of deformation mechanisms and slip systems in quartz, as the control exerted by these factors is probably more effective than previously thought based on models built on experimentally deformed quartzites at various temperatures and/or natural pure quartz mylonites produced at different metamorphic grades.

ACKNOWLEDGMENTS

The paper has greatly benefitted from thoughtful and constructive reviews by Chiara Frassi and Michele Marroni, as well as from the useful comments by Ofioliti Editor Luca Pandolfi. SEM-EBSD analyses were carried out at the John de Laeter Centre, Curtin University of Technology. Financial and technical support from Curtin University of Technology and the University of Naples Federico II are gratefully acknowledged.

REFERENCES

Allmendinger R.W., Cardozo N. and Fisher D.M., 2012. Structural geology algorithms: Vectors and tensors. Cambridge University Press. 286 pp.

Ballèvre M. and Merle O., 1993. The Combin fault: compressional reactivation of a Late Cretaceous-Early Tertiary detachment fault in the Western Alps. Schweiz. Mineral. Petrogr. Mitt., 73 (2): 205-227.

Barnicoat A.C. and Fry N., 1986. High-pressure metamorphism of the Zermatt-Saas ophiolite zone, Switz.. J. Geol. Soc., 143 (4): 607-618.

Bearth P.P., 1967. Die Ophiolithe der Zone von Zermatt-Saas Fee. Beitr. Geol. Karte Schweiz, N.F. 132, 1-130.

Bestmann M. and Pennacchioni G., 2015. Ti distribution in quartz across a heterogeneous shear zone within a granodiorite: The effect of deformation mechanism and strain on Ti resetting. Lithos, 227: 37-56.

Blacic J.D., 1975. Plastic-deformati on mechanisms in quartz: The effect of water. Tectonophysics, 27 (3): 271-294.

Blumenfeld P,, Mainprice D. and Bouchez J.L., 1986. C-slip in quartz from subsolidus deformed granite. Tectonophysics, 127 (1-2): 97-115.

Boneh Y. and Skemer P., 2014. The effect of deformation history on the evolution of olivine CPO. Earth Planet. Sci. Lett., 406: 213-222.

Cardozo N. and Allmendinger R.W., 2013. Spherical projections with OSXStereonet. Comput. Geosci., 51: 193-205.

Carreras J. and Celma A.G., 1982. Quarz of C-Axis fabric variation at the margins of a shear zone developed in shists from cap de Creus (Spain). Acta Geol. Hisp., 17 (3): 137-149.

Cross A.J., Kidder S. and Prior D.J., 2015. Using microstructures and TitaniQ thermobarometry of quartz sheared around garnet porphyroclasts to evaluate microstructural evolution and constrain an Alpine Fault Zone geotherm. J. Struct. Geol., 75: 17-31.

Dal Piaz G.V., 1999. The Austroalpine-Piedmont nappe stack and the puzzle of Alpine Tethys. Memorie di Scienze Geologiche, 51(1): 155-76.

Dal Piaz G.V. and Ernst W.G., 1978. Areal geology and petrology of eclogites and associated metabasites of the Piemonte ophiolite nappe, Breuil - St. Jacques area, Italian Western Alps. Tectonophysics, 51 (1): 99-126.

Dal Piaz G.V., Bistacchi A. and Massironi M., 2003. Geological outline of the Alps. Episodes, 26 (3): 175-180.

Ellis A.C., Barnicoat A.C. and Fry N., 1989. Structural and metamorphic constraints on the tectonic evolution of the upper Pennine Alps. Geol. Soc. London Spec. Publ., 45 (1): 173-188.

ten Grotenhuis S.M., Trouw R.A. and Passchier C.W., 2003. Evolution of mica fish in mylonitic rocks. Tectonophysics, 372 (1): 1-21.

Heilbronner R. and Tullis J., 2006. Evolution of c axis pole figures and grain size during dynamic recrystallization: Results from experimentally sheared quartzite. J. Geophys. Res. Solid Earth, 111, B10202.

Hippertt J.F., 1994. Microstructures and c-axis fabrics indicative of quartz dissolution in sheared quartzites and phyllonites. Tectonophysics, 229 (3): 141-163.

Hobbs B.E., 1985. The geological significance of microfabric analysis. In: Preferred orientation in deformed metals and rocks: An introduction to modern texture analysis (Ed H. R. Wenk), Academic Press, San Diego, 463-484.

Kilian R., Heilbronner R. and Stünitz H., 2011. Quartz grain size reduction in a granitoid rock and the transition from dislocation to diffusion creep. J. Struct. Geol., 33 (8): 1265-1284.

Kruhl J.H., 1996. Prism- and basal-plane parallel subgrain boundaries in quartz: A microstructural geothermobarometer. J. Metam. Geol., 14 (5): 581-589.

Law R.D., 2014. Deformation thermometry based on quartz c-axis fabrics and recrystallization microstructures: A review. J. Struct. Geol., 66: 129-161.

Law R.D., Schmid S.M. and Wheeler J., 1990. Simple shear deformation and quartz crystallographic fabrics: a possible natural example from the Torridon area of NW Scotland. J. Struct. Geol., 12 (1): 29-45.

Lister G.S. and Hobbs B.E., 1980. The simulation of fabric development during plastic deformation and its application to quartzite: the influence of deformation history. J. Struct. Geol., 2 (3): 355-370.

Little T.A., Prior D.J., Toy V.G. and Lindroos Z.R., 2015. The link between strength of lattice preferred orientation, second phase content and grain boundary migration: A case study from the Alpine Fault zone, New Zealand. J. Struct. Geol., 81: 59-77.

Mazzoli S., Martín-Algarra A., Reddy S.M., Sánchez-Vizcaíno V.L., Fedele L. and Noviello A., 2013. The evolution of the footwall to the Ronda subcontinental mantle peridotites: insights from the Nieves Unit (western Betic Cordillera). J. Geol. Soc., 170 (3): 385-402.

Menegon L., Pennacchioni G., Heilbronner R. and Pittarello L., 2008. Evolution of quartz microstructure and c-axis crystallographic preferred orientation within ductilely deformed granitoids (Arolla unit, Western Alps). J. Struct. Geol., 30 (11): 1332-1347.

Milnes A.G., Greller M. and Müller R., 1981. Sequence and style of major post-nappe structures, Simplon - Pennine Alps. J. Struct. Geol., 3(4): 411-420.

Muto J., Hirth G., Heilbronner R. and Tullis J., 2011. Plastic anisotropy and fabric evolution in sheared and recrystallized quartz single crystals. J. Geophys. Res., Solid Earth, 116(B2).

Passchier C.W. and Trouw R.A., 1998. Dilatation sites: Fibrous veins, strain shadows, strain fringes and boudins. In: Microtectonics (vol. 256) 131-151, Springer, Berlin.

Pennacchioni G., Menegon L., Leiss B., Nestola F. and Bromiley G., 2010. Development of crystallographic preferred orientation and microstructure during plastic deformation of natural coarse-grained quartz veins. J. Geophys. Res., Solid Earth, 115(B12).

Peternell M., Hasalová P., Wilson C.J., Piazolo S. and Schulmann K., 2010. Evaluating quartz crystallographic preferred orientations and the role of deformation partitioning using EBSD and fabric analyser techniques. J. Struct. Geol., 32 (6): 803-817.

Platt J.P., 1986. Dynamics of orogenic wedges and the uplift of high-pressure metamorphic rocks. Geol. Soc. Am. Bull., 97 (9):1037-1053.

Pleuger J., Roller S., Walter J.M., Jansen E. and Froitzheim N., 2007. Structural evolution of the contact between two Penninic nappes (Zermatt-Saas zone and Combin Zone, Western Alps) and implications for the exhumation mechanism and palaeogeography. Intern. J. Earth Sci., 96 (2): 229-252.

Price G.P., 1985. Preferred orientations in quartzites. In: Preferred orientation in deformed metals and rocks: An introduction to modern texture analysis (Ed H.R. Wenk), Academic Press, San Diego, 385-406.

Ramsay J.G. and Huber M.I., 1987. The techniques of modern structural geology: Folds and fractures (Vol. 2). Academic press. 700 pp.

Reddy S.M. and Buchan C., 2005. Constraining kinematic rotation axes in high-strain zones: a potential microstructural method?. In: Deformation Mechanism, Rheology and Tectonics: from Minerals to the Lithosphere (Eds. G. Gapais, J.P. Brun & P.R. Cobbold),. Geol. Soc. London Spec. Publ., 243 (1): 1-10.

Reddy S.M., Timms N.E., Pantleon W. and Trimby P., 2007. Quantitative characterization of plastic deformation of zircon and geological implications. Contrib. Miner. Petrol., 153 (6): 625-645.

Reddy S.M., Wheeler J., Butler R.W., Cliff R.A., Freeman S., Inger S., Pickles C. and Kelley S.P., 2003. Kinematic reworking and exhumation within the convergent Alpine Orogen. Tectonophysics, 365 (1): 77-102.

Reddy S.M., Wheeler J. and Cliff R.A., 1999. The geometry and timing of orogenic extension: an example from the Western Italian Alps. J. Metam. Geol., 17: 573-590.

Reinecke T., 1991. Very-high-pressure metamorphism and uplift of coesite-bearing metasediments from the Zermatt-Saas zone, Western Alps. Eur. J. Miner., 3(1): 7-18.

Schmid S.M. and Casey M., 1986. Complete fabric analysis of some commonly observed quartz caxis patterns. Mineral and rock deformation: Laboratory studies: The Paterson Volume, (Eds. B.E. Hobbs & H.C. Heard), American Geophysical Union, Geophysical Monograph vol. 36. Washington, DC, USA, 263-286.

Stipp M., Stuènitz H., Heilbronner R. and Schmid S.M., 2002 The eastern Tonale fault zone: a 'natural laboratory'for crystal plastic deformation of quartz over a temperature range from 250 to 700 C°. J. Struct. Geol., 24 (12): 1861-1884.

Toy V.G., Prior D.J. and Norris R.J., 2008. Quartz fabrics in the Alpine Fault mylonites: Influence of pre-existing preferred orientations on fabric development during progressive uplift. J. Struct. Geol., 30 (5): 602-621.

Tullis J., 1977. Preferred orientation of quartz produced by slip during plane strain. Tectonophysics, 39 (1-3): 87-102.

Tullis J., Christie J.M. and Griggs D.T., 1973. Microstructures and preferred orientations of experimentally deformed quartzites. Geol. Soc. Am. Bull., 84 (1): 297-314.

Vitale S. and Mazzoli S., 2008. Heterogeneous shear zone evolution: the role of shear strain hardening/softening. J. Struct. Geol., 30 (11): 1383-1395.

Vitale S. and Mazzoli S., 2010. Strain analysis of heterogeneous ductile shear zones based on the attitudes of planar markers. J. Struct. Geol., 32 (3): 321-329.

Wheeler J., Reddy S.M. and Cliff R.A., 2001. Kinematic linkage between internal zone extension and shortening in more external units in the NW Alps. J. Geol. Soc., 158 (3): 439-443.

Received, September 28, 2016
Accepted, November 21, 2016